PFC/JA-90-25

A High–Voltage Modulator for High–Power RF Source Research

Mulligan, W., Chen, S.C., Bekefi, G.,
B.G. Danly, Temkin, R.J.

Plasma Fusion Center
Massachusetts Institute of Technology
Cambridge, MA 02139

July 1990

This work was supported by Harry Diamond Labs (Army) Contract DAAL02–89–K–0084.

A HIGH-VOLTAGE MODULATOR FOR HIGH-POWER RF SOURCE RESEARCH

W. Mulligan, S.C. Chen, G. Bekefi, B.G. Danly, and R.J. Temkin

Plasma Fusion Center
Massachusetts Institute of Technology, Cambridge, MA 02139

Abstract

We present the design, construction, and operating results of a high voltage modulator system capable of generating 700 kV, 2.5 μs pulses at 5 pps into a load of 900 Ω. The modulator is used to energize a variety of high power microwave devices requiring voltage stability and reproducibility. Voltage ripple is less than 0.2% during the 1.0 μs flat top, with a shot-to-shot voltage variation of less than 0.1%. The primary circuit consists of two seven-stage tunable Rayleigh-type pulse forming networks (PFNs) connected in parallel with a total impedance of 2.25 Ω, a total capacitance of 0.56 μF, and a total inductance of 2.8 μH. The PFN is charged by a highly stable 80 kV capacitor charging power supply (0.1% RMS voltage ripple) at a rate of 10 kJ/sec. The total energy stored (1.5 kJ) is released through an ITT F-187 thyratron into a 20:1 pulse transformer, which generates 700 kV, 2.5 μs pulses. By changing the transformer, we have also obtained 250 kV, 1.7 kA pulses for driving low impedance relativistic magnetron diodes. The flat-top voltage generated by the modulator is highly desirable for driving rf sources requiring high quality electron beams, such as free-electron lasers (FEL) and cyclotron auto-resonance masers (CARM). The modulator performance in our relativistic magnetron and CARM experiments is described.

I. Introduction

The generation of coherent electromagnetic radiation using high energy electrons in vacuum relies on the synchronism between the interacting electron bunch and wave to facilitate net energy exchange. To obtain high power rf with high extraction efficiency, usually it is important to use electron beams of high quality, namely with high current, low emittance, and small energy spread. The MIT 700 kV modulator has demonstrated the capability of producing tunable high voltage flat-top pulses, suitable for driving a variety of rf sources. A necessary requirement of this modulator is that it should be able to supply highly stable pulses to different experiments, each having different voltage and current requirements. For applications involving time-dependent load impedance, such as in relativistic magnetrons, special design considerations are required. Even under the most hostile operating condition, as in the case of a shorting relativistic magnetron load, the modulator successfully handled the reflected power. A block diagram of the modulator is shown in Fig. 1 and a schematic diagram in Fig. 2.

II. Modulator Description

The modulator has the following parameters:

Peak Pulse Power	500 MW
Pulse Repetition Frequency	5 pps
Output Pulse Voltage	700 kV
Output Impedance	900 Ω
Pulse to Pulse Regulation	0.1%
Pulse Ripple, 1 μs flat-top	0.2%

The PFN is charged by a 10 kJ/sec, 0–80 kV resonant inverter power supply, with 0.1% regulation, giving a pulse repetition frequency of 5 pps. The modulator switch is an ITT F–187 thyratron rated for 75 kV and 20 kA. Another F–187 is used for an end-of-line clipper with a series 1.6 Ω resistor to absorb the reflected energy when a short circuit occurs.

The complete modulator is submersed in a stainless steel tank 8 ft. long by 4 ft. wide by 4 ft. deep which is filled with transformer oil (Shell DIALAX). At the output end of the modulator the tank has two 18 inch ports with O–ring flanges for attaching the cathode stalks or electron guns employed in different experiments. All high voltage connections to the experiments are made in oil. The tank is completely covered and interlocked for personnel safety. The oil in the tank can be pumped through a three-stage filtration system.

The transformer has a 20:1 turns ratio with bifilar windings on the secondary for supplying filament power to the electron guns used as the load. The load used to test the modulator and to use in parallel with high impedance experiments is a 975 Ω resistor, capable of dissipating 5 kW, made by the Stackpole Co. The resistor is made with thirty 30 Ω disks all bolted together with a 0.5 inch phenolic rod. Each disk is 1 inch thick and 4.4 inches in diameter. After immersed in oil for a period of time, the resistance of the resistor increased from the original 900 Ω to 975 Ω.

The PFN impedance of 2.25 Ω is generated by using two Rayleigh type, 4.5 Ω PFNs in parallel. Each PFN has 7 sections and each section has an inductance variable between 0.2 and 1.2 μH. The inductance can be changed in steps and also fine tuned between steps. The capacitors are 40 nF each with low internal inductance and a rated voltage of 80 kV, manufactured by Maxwell Laboratories. The maximum stray inductance external to the PFN for it to retain tunability is 1.3 μH.

The sections of the PFN are separated by 6 inches to minimize mutual inductance between coils. The calculated mutual inductance between coils is 30 nH. With the Rayleigh-type PFN the pulse width can be reduced, if desired, by removing sections.

The PFN is charged with a voltage regulated constant energy, 10 kJ/sec, power supply. The power supply has two modes of operation, continuous run and command arm/fire. We use the arm and fire mode in the experiment. Figure 3 shows the charging-firing cycle for three different charging voltages (40, 44, 48 kV). Upon receiving the charge command, the voltage is charged up linearly to the desired value and held high until the firing pulse dumps the energy.

The clipper thyratron has very low inductance, 75 nH, and is rated for 75 kV at 20 kA. The low inductance (thyratron inductance plus stray inductances) is very important since it determines how fast the reflected energy can be removed. A critical rating of the switch thyratron is its peak inverse voltage, immediately after forward conduction, which for the F–187 is 10 kV. If the reverse voltage is allowed to exceed 10 kV, arcing may occur which is very harmful to the thyratron and may cause its demise.

Since the experiments that this modulator will be driving run at a low repetition frequency, it was decided to use a voltage regulated, resonant inverter constant energy power supply rather than resonant charging with de–Qing. The voltage waveshape on the PFN is shown in Fig. 4.

The modulator PFN is discharged through an ITT F-187 thyratron into a 1:20 pulse transformer which gives an output voltage up to 700 kV into the load. When an experiment with an impedance higher than 900 Ω is used an appropriate resistor is used in parallel to bring the total secondary load close to 900 Ω. If the experimental load is less than 900 Ω, any reflected power is absorbed by the clipper circuits. The pulse shape of the PFN is easily varied to give any desired shape to the top of the pulse. The modulator functioned as designed and has been tested to 625 kV on a 975 Ω load. The output waveform is shown in Fig. 4. For this test, the charging voltage was 61 kV.

At high voltages, the relativistic magnetron tends to short circuit a few hundred nanoseconds into the pulse [1], the clipper circuits (thyratron plus diode) then absorb all of the reflected energy. The thyratron clipper is automatically triggered and works very well provided the external inductance is kept low. The solid state clipper that is used in parallel with the thyratron (see Fig. 2) has three EDI model ED-2212 diode stacks in series with a total inverse voltage rating of 225 kV and a 50 kA peak current rating. The diode stack successfully takes out part of the reflected power as designed. However, if the diode stack is used alone – without the thyratron –, it is too slow to absorb all of the reflected energy.

A capacitive voltage divider is used to measure the high voltage pulse on the secondary of the pulse transformer. The capacitive voltage divider is a Stangenes model CVD-800 rated for a peak voltage of 800 kV and 12200:1 voltage division. The results using the probe have been very satisfactory although care has to be taken not to change cable length after the probe has been calibrated. A second method used to measure the high voltage pulse is to measure the current through the 975 Ω secondary load using a Rogowski current transformer. This method proves to be difficult to calibrate because the resistance value of the carbon resistor that we use for a load varies with voltage at these high voltages.

III. Operation with a Relativistic Magnetron

The modulator has been used to drive a high power, long pulse relativistic magnetron experiment [1,2,3]. The μs pulses are more than 20 times longer than in all previous relativistic magnetron experiments and it is essential for injection locking of high power oscillators. Interesting diode impedance variations were observed in the experiment [1], which owe their origin to the emission characteristics of the cold cathode in the relativistic magnetron diode under crossed electric, magnetic and strong rf fields. The magnetron impedance Z of a cold-cathode field-emission system is determined by the interplay between the following processes: (1) the nonlinear field emission process under the applied anode voltage V , and (2) the magnetic insulation process under the applied transverse magnetic field B. The impedance can be written as a function of the relevant variables:

$$Z = Z(V,\ B,\ ,g, \ldots) \tag{1}$$

where g is the anode-cathode gap. It should be noted that the anode voltage, in turn, depends on the magnetron impedance

$$V = V_{matched} \cdot \frac{2\frac{Z}{Z_{p.s.}}}{(1 + \frac{Z}{Z_{p.s.}})} \tag{2}$$

where $Z_{p.s.}$ is the power supply impedance , and $V_{matched}$ is the anode voltage under matched condition $Z = Z_{p.s.}$. The nonlinear interdependence between Z and V (Eqs. (1) and (2)) is an interesting phenomenon deserving further experimental and theoretical study. Under operating conditions, the presence of the strong electromagnetic field, whose electric field component is comparable to the applied DC field, further complicates the interaction.

Details of the experimental setup were reported elsewhere [1,3]. We describe here only those results relevant to the modulator performance. During the relativistic magnetron interaction, due to the expanding cathode plasma, the effective anode-cathode gap reduces as a function of time. Thus, more and more current is drawn, and the impedance is monotonically reduced during the pulse. This fact manifests itself through a voltage droop and a current increase in the output waveform (Fig. 5). To maintain the resonance between the electrons and waves (Buneman-Hartree condition), it is important that the voltage pulse is held flat. We have demonstrated the capability to tune the PFN so that under matched conditions it produces a rising slope large enough to compensate for the magnetron voltage droop under running condition.

IV. Operation with Cyclotron Autoresonance Maser and Free Electron Laser

The 700 kV modulator is also in use for both cyclotron autoresonance maser (CARM) and free–electron laser (FEL) experiments at the MIT Plasma Fusion Center. The pulse transformer secondary may be connected to either the relativistic magnetron or to the electron gun used for the CARM/FEL experiments. A Ka–band CARM oscillator experiment which utilizes a SLAC 5045 klystron gun operating at up to 315 kV has been carried out [4,5], and a new 700 kV, 0.27 μP diode gun built by Thomson–CSF of France has been installed on the modulator for FEL and CARM studies.

High peak power CARM or FEL amplifiers operating in the 11–17 GHz frequency range are attractive rf sources for powering the next generation of linear colliders [4].

The long pulse width (relative to linear induction accelerators) and low voltage ripple obtained with this type of pulse modulator are important for achieving the rf phase stability required of rf–accelerator drivers [6]. The rf output from modulator–driven CARM or FEL amplifiers with microsecond pulse lengths can be pulse–compressed to obtain higher peak powers in shorter pulses if necessary [7].

High voltage modulator–driven CARMs or FELs may also be attractive as sources of high average power in the 140–280 GHz frequency range for use in electron–cyclotron resonance heating (ECRH) of fusion plasmas. Burst mode operation of modulator driven CARMs or FELs with 0.5–1 MeV beam energies, currents of ~1 kA, and duty factors of 0.1% to 0.5% may be attractive for megawatt average power level ECRH sources.

V. Discussion

The modulator has performed very satisfactorily under all types of loads. The electron gun in the CARM oscillator experiment behaves like a matched load, and the modulator delivered flat voltage pulses reliably. When used in the cold-cathode relativistic magnetron experiment, the modulator performed as designed even with the time-dependent load impedance. When the magnetron impedance collapsed to a very low value before the end of the modulator pulse, the modulator successfully absorbed the reflected power.

Several improvements to this modulator are planned. In order to drive rf sources of different characteristic impedances, the pulse transformer will be modified into a multi–impedance transformer with four different impedance taps (20:1, 12:1, 8:1, 5:1). More efficient power transfer from the modulator to the rf sources is expected. The clipper circuits will be greatly simplified with the installation of low inductance solid state diodes which allow us to avoid the clipper thyratron and its complex peripheral circuitry.

VI. Acknowledgement

This work was supported by Strategic Defense Initiative Organization, Office of Innovative Science and Technology, and managed by Harry Diamond Laboratories.

Reference

[1] S.C. Chen, G. Bekefi, and R. Temkin, "Operation of a long pulse relativistic magnetron in a phase-locking system," *Proc. SPIE*, vol. 1226, pp 36-43, 1990.

[2] S.C. Chen and G. Bekefi, "Relativistic magnetron research," N. Rostoker, Editor, *Proc. SPIE*, vol. 873, pp 18-22, 1988.

[3] S.C. Chen, G. Bekefi, R. Temkin, and C. de Graff, "Proposed injection locking of a long pulse relativistic magnetron," H.E. Brandt, Editor, *Proc. SPIE*, vol. 1061, pp. 157-160, 1989.

[4] B.G. Danly, J.S. Wurtele, K.D. Pendergast, and R.J. Temkin, "CARM driver for high frequency rf accelerators," *Proceedings of the 1989 IEEE Particle Accelerator Conference*, vol. 1, pp.223-225, 1989.

[5] K.D. Pendergast, et al., in preparation.

[6] P.B. Wilson, "High pulse power rf sources for linear colliders," SLAC–PUB–3227, 1983.

[7] Z.D. Farkas and J.N. Weaver, "RF pulse compression development," SLAC–AP–59, 1987.

Figure Caption

Fig. 1 Block diagram of the MIT 700 kV modulator

Fig. 2 Schematic diagram of the MIT 700 kV modulator

Fig. 3 Charging-firing cycle for three different charging voltages (40, 44, 48 kV). Upon receiving the charge command, the voltage is charged up linearly to the desired value and held high until the firing pulse dumps the energy. Time – 50 ms/div, voltage – 10 kV/div.

Fig. 4 Secondary voltage waveform across a matched load. With a charging voltage of 61 kV, the output flat-top voltage is 625 kV. Time – 500 ns/div, voltage – 97.5 kV/div.

Fig. 5 Voltage and current waveforms of a cold-cathode relativistic magnetron. The modulator was charged up to 20 kV, and a 8:1 pulse transformer is used. Due to the expanding cathode plasma, more and more current is drawn and the impedance is monotonically reduced during the pulse. This fact manifests itself through a voltage droop (lower trace) and a current increase (upper trace). Time – 500 ns/div, voltage – 19.2 kV/div, current 200 A/div.

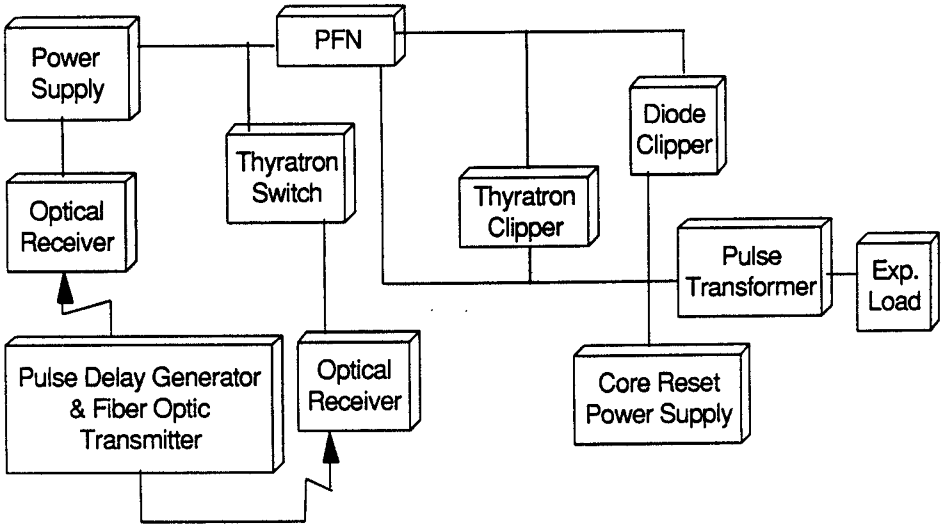
Power Supply
PFN
Thyratron Switch
Thyratron Clipper
Diode Clipper
Optical Receiver
Pulse Transformer
Exp. Load
Pulse Delay Generator & Fiber Optic Transmitter
Optical Receiver
Core Reset Power Supply

Fig. 1

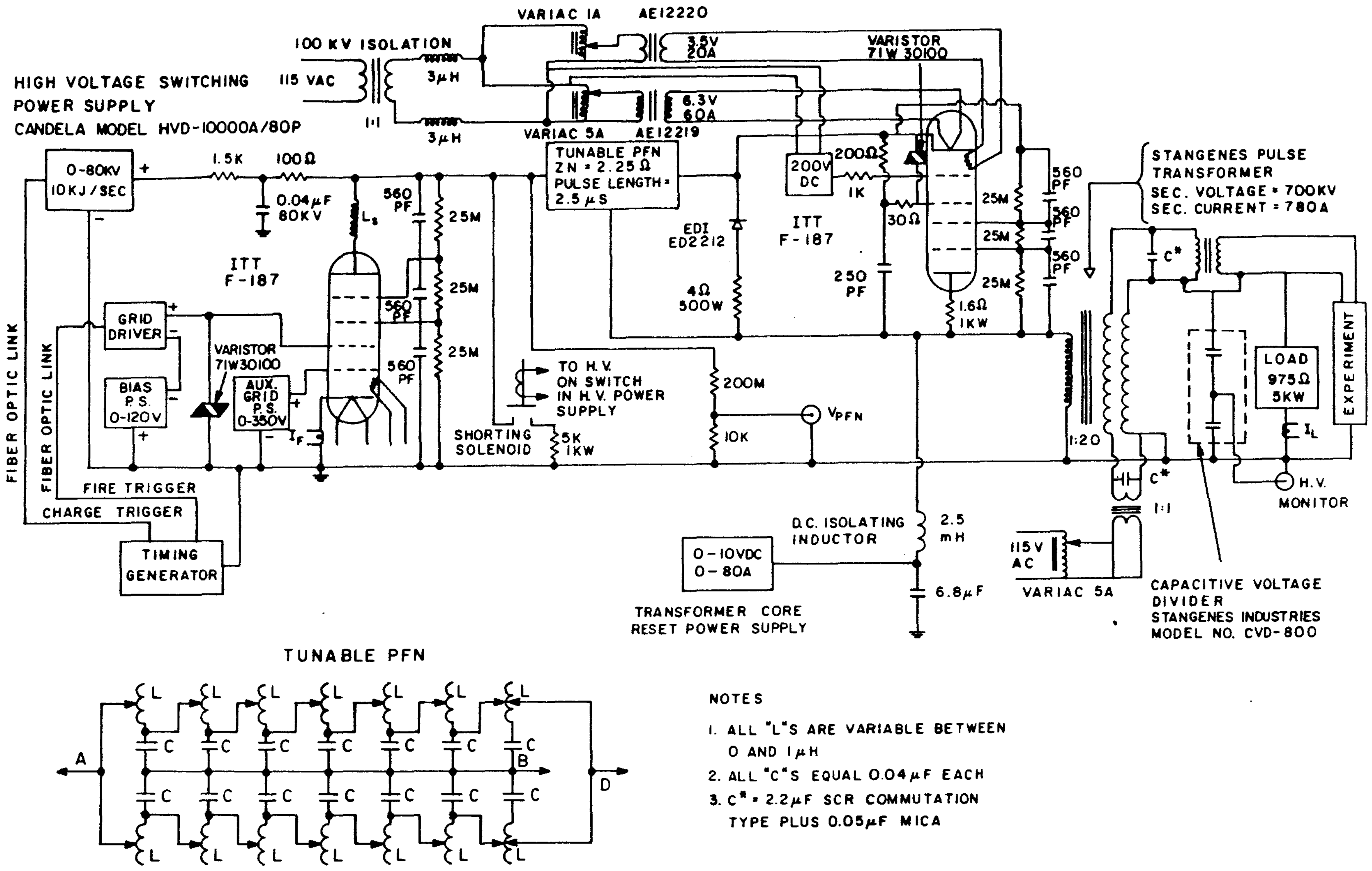

NOTES

1. ALL "L"S ARE VARIABLE BETWEEN 0 AND 1μH
2. ALL "C"S EQUAL 0.04μF EACH
3. C* = 2.2μF SCR COMMUTATION TYPE PLUS 0.05μF MICA

Fig. 2

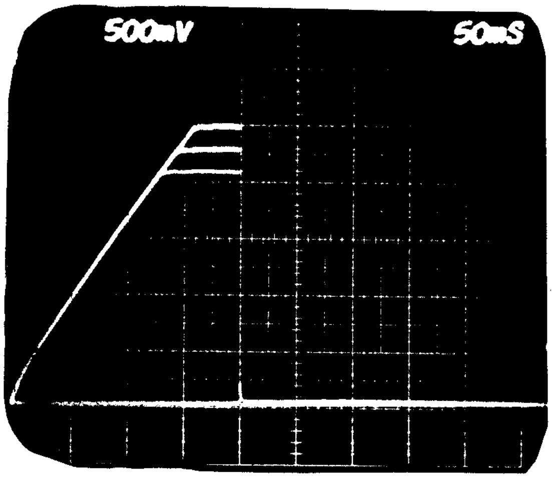

Fig. 3

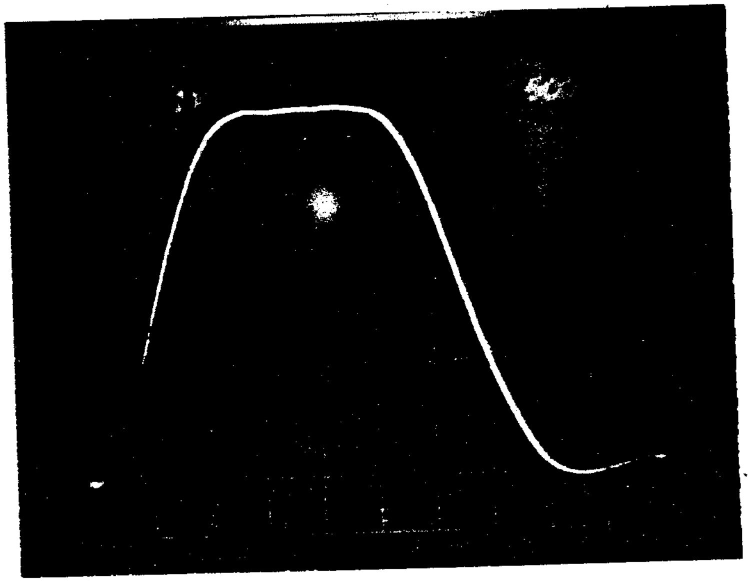

Fig. 4

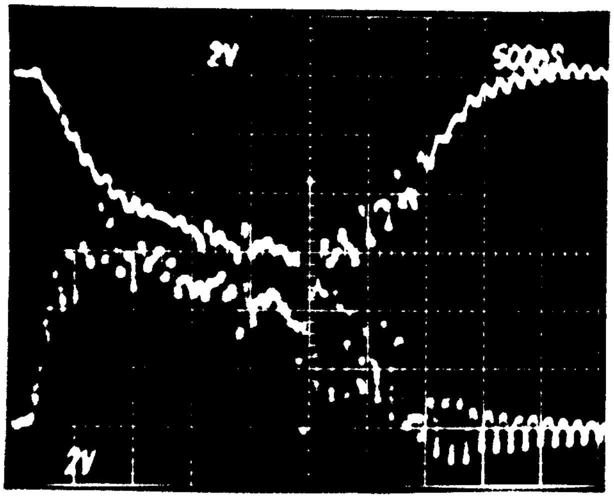

Fig. 5